Graded expression of zinc-responsive genes through two regulatory zinc-binding sites in Zur

Jung-Ho Shin[a,1], Hoi Jong Jung[b,1], Young Jun An[b], Yoo-Bok Cho[a], Sun-Shin Cha[b,c,2], and Jung-Hye Roe[a,2]

[a]Laboratory of Molecular Microbiology, School of Biological Sciences, and Institute of Microbiology, Seoul National University, Seoul 151-742, Republic of Korea; [b]Marine Biotechnology Research Center, Korea Ocean Research and Development Institute, Ansan 426-744, Republic of Korea; and [c]Department of Marine Biotechnology, University of Science and Technology, Daejeon 305-333, Republic of Korea

Edited by John D. Helmann, Cornell University, Ithaca, NY, and accepted by the Editorial Board February 9, 2011 (received for review December 1, 2010)

Zinc is one of the essential transition metals in cells. Excess or lack of zinc is detrimental, and cells exploit highly sensitive zinc-binding regulators to achieve homeostasis. In this article, we present a crystal structure of active Zur from *Streptomyces coelicolor* with three zinc-binding sites (C-, M-, and D-sites). Mutations of the three sites differentially affected sporulation and transcription of target genes, such that C- and M-site mutations inhibited sporulation and derepressed all target genes examined, whereas D-site mutations did not affect sporulation and derepressed only a sensitive gene. Biochemical and spectroscopic analyses of representative metal site mutants revealed that the C-site serves a structural role, whereas the M- and D-sites regulate DNA-binding activity as an on-off switch and a fine-tuner, respectively. Consistent with differential effect of mutations on target genes, zinc chelation by TPEN derepressed some genes (*znuA, rpmF2*) more sensitively than others (*rpmG2*, SCO7682) in vivo. Similar pattern of TPEN-sensitivity was observed for Zur-DNA complexes formed on different promoters in vitro. The sensitive promoters bound Zur with lower affinity than the less sensitive ones. EDTA-treated apo-Zur gained its DNA binding activity at different concentrations of added zinc for the two promoter groups, corresponding to free zinc concentrations of 4.5×10^{-16} M and 7.9×10^{-16} M for the less sensitive and sensitive promoters, respectively. The graded expression of target genes is a clever outcome of subtly modulating Zur-DNA binding affinities in response to zinc availability. It enables bacteria to detect metal depletion with improved sensitivity and optimize gene-expression pattern.

ferric uptake regulator | graded transcription regulation | regulatory metal

Various transition metal ions are essentially required for cell growth and survival because they stabilize the folded conformations or mediate chemical reactions of metalloproteins, which constitute about one-third of all proteins (1, 2). Zinc is an abundant transition metal that serves as a cofactor for diverse enzymes and regulatory proteins. It is estimated that about 5% to 10% of all proteins predicted from the genomes of all three domains of life are zinc-proteins (3). In *Escherichia coli* the total zinc content inside the cell is reported to be in the millimolar range, whereas the zinc-responsive transcriptional regulators respond to femtomolar (fM) range of free zinc, reflecting its dramatic zinc-binding capacity and sensitive regulation (4). In bacteria, zinc homeostasis is regulated primarily by zinc-specific regulators of the ferric uptake regulator (Fur) family (Zur), MerR family (ZntR), and ArsR/SmtB family (SmtB, CzrA) (5). In *E. coli*, zinc uptake genes are repressed by Zur, whereas export genes are activated by ZntR, in femtomolar concentration ranges of free zinc (4). In many bacteria, zinc depletion causes inactivation of zinc-specific Zur to derepress zinc transporter genes (6). In Gram-positive bacteria, genes for zincless ribosomal proteins are derepressed to replace zinc-bound paralogs as a way of mobilizing zinc (7–12). Coelibactin, a putative zincophore, has been recently reported to be regulated by Zur in *Streptomyces coelicolor* (13, 14). In addition, Zur can also act as a direct activator to induce a zinc-export system in *Xanthomonas campestris* (15).

The Fur family members, widely distributed among bacteria, are versatile metalloregulators that respond to diverse transition metals, such as iron, zinc, manganese, and nickel (16, 17). The mechanisms of metal-specificity and metal-mediated activity modulation have been extensively investigated, revealing some common and specific principles among members of this family. Crystal structures of several metal-bound Fur regulators have been reported for iron-responsive Fur from *Pseudomonas aeruginosa* (*Pa*Fur) (18) and *Vibrio cholerae* (*Vc*Fur) (19), zinc-responsive Zur from *Mycobacterium tuberculosis* (*Mt*Zur) (20), nickel-responsive Nur from *S. coelicolor* (*Sc*Nur) (21), and peroxide-sensing PerR from *Bacillus subtilis* (*Bs*PerR) (22). All of the available structures demonstrate that the Fur family members are homodimeric and each monomer consists of an N-terminal DNA-binding (DB) domain, a C-terminal dimerization (D) domain, and a hinge loop between the two. Metal-bound functional proteins usually exhibit two metal-binding sites. One site lies in the inter-domain hinge-loop region (M-site). The other resides in the D-domain, constructed by either four conserved cysteines near the C terminus (C-site) or residues at the surface of the D-domain pointing toward the hinge region (D-site). Structural comparison between inactive apo- and metallated active forms of *Bs*PerR suggested that regulatory metal binding causes DB-domains to swing around the hinge region with respect to the D-domain, from an open (swung-out) to closed (converged) conformations (22–24). This process leads to a model that the rearrangement of DB-domains by binding a regulatory metal in the hinge region is responsible for the allosteric transition of all Fur family regulators, from the inactive open conformation to the active closed one (23).

In this respect, the presence of three metal (Zn) binding sites determined from the structural study of *Mt*Zur (20) has been hard to interpret. The reported structure assumes an open dimeric conformation inadequate for DNA-binding, despite zinc occupation of the M-site in the hinge region. Here, we present the active conformation of zinc-bound Zur that assumes the closed conformation suitable for DNA-binding, on the basis of the 2.4 Å resolution crystal structure of *S. coelicolor* Zur (*Sc*Zur). Through mutational and functional studies, we reveal that *Sc*Zur contains two regulatory metal sites (M- and D-sites) in addition to one structural one (C-site). Functional role of two regulatory

Author contributions: J.-H.S., H.J.J., Y.-B.C., S.-S.C., and J.-H.R. designed research; J.-H.S., H.J.J., Y.J.A., and S.-S.C. performed research; J.-H.S. and J.-H.R. contributed new reagents/analytic tools; J.-H.S., H.J.J., Y.J.A., Y.-B.C., S.-S.C., and J.-H.R. analyzed data; and J.-H.S., S.-S.C., and J.-H.R. wrote the paper.

The authors declare no conflict of interest.

This article is a PNAS Direct Submission.

J.D.H. is a guest editor invited by the Editorial Board.

Data deposition: The sequences in this paper have been deposited in PDB (Code number 3MWM).

[1]J.-H.S. and H.J.J. contributed equally to this work.

[2]To whom correspondence may be addressed. E-mail: jhroe@snu.ac.kr or chajung@kordi.re.kr.

This article contains supporting information online at www.pnas.org/lookup/suppl/doi:10.1073/pnas.1017744108/-/DCSupplemental.

MICROBIOLOGY

metal sites and its implication for differential expression of Zur target genes are presented.

Results

Overall Structure of *Sc*Zur with a Closed Conformation. *Sc*Zur is a homodimer with a modular architecture similar to previously determined Fur-family members. DB-domain (residues 1–77) with the winged helix motif consists of a three-helical bundle and a two-stranded sheet (Fig. 1*A*, H1–H3 and S1–S2). The D-domain (residues 86–145) has a three-stranded sheet (Fig. 1*A*, S3–S5) with a long helix (Fig. 1*A*, H4) and a short 3_{10} helix (Fig. 1*A*, H5) on opposite edges of the sheet, respectively. In the dimeric structure, two D-domains build up the dimeric core where two three-stranded sheets from each D-domain are combined to form a six-stranded intermolecular sheet. Two DB-domains are positioned below the dimeric core (Fig. 1*A*), generating the arch shape of the dimeric *Sc*Zur.

The anomalous scattering from zinc was exploited to determine the number and the position of zinc sites. There are three zinc-binding sites in each monomer of *Sc*Zur; site 1 (M), site 2 (C), and site 3 (D) (Fig. 1*B*). Each site accommodates a zinc ion with the tetrahedral geometry. The M-site at the domain interface is formed by Asp65 from the DB-domain (S1), Cys79 and His85 from the hinge loop, and His87 from the D-domain (S3). The C-site is constructed by four cysteines (Cys90, Cys93, Cys130, and Cys133) at one end of the D-domain. The D-site is located at the other end of the D-domain, where His84, His86, Glu105, and His122 participate in zinc coordination.

Effect of Mutations in Sporulation of *S. coelicolor*. To find the contribution of various residues, especially metal-coordinating ones identified by the crystal structures of *Sc*Zur and other Fur family members, we made substitution mutants of *Sc*Zur. Cysteine residues were changed to serines, and others were changed to alanines to create variants such as E28A, F29A, R30A, H36A, H41A, D65A, R68A, E71A, R77A, C79S, H84A, H85A, H86A, H87A, C90S, C93S, E98A, E105A, H115A, H122A, C130S, and C133S. The position of 22 mutated residues was presented in the 3D structure (Fig. 2*A*) and in the primary sequence of *Sc*Zur aligned with other Fur family members (*SI Appendix*, Fig. S1).

In contrast to wild-type *S. coelicolor*, which forms gray-green spores on soya flour mannitol (SFM) plates, the *Δzur* mutant did not sporulate, forming only aerial mycelia of a white puffy appearance. This phenotype has been proposed to result partly from overexpression of a Zur target gene SCO7682, encoding a putative zincophore called coelibactin (13, 14). When the wild-type *zur* gene was introduced to *Δzur* on a pSET162-based vector, it enabled sporulation, restoring gray-green colors of the colony (Fig. 2*B*, WT). We used this complementation analysis as a way to judge functionality of Zur in *S. coelicolor*. Introduction of various mutant genes revealed that some mutations did not restore sporulation, suggesting that they lost functionality with respect to sporulation and possibly SCO7682 regulation. The nonfunctional mutations were F29A, R77A, C79S, H85A, H87A, C90S, C93S, C130S, and C133S, retaining white colors of the colonies. The other mutations appeared as nearly functional as the wild-type gene, showing light to deep gray-green colors. The nonfunctional mutations all resided at the C- or M-site, except for F29A and R77A, which are at the interdomain interface and thus very likely to affect domain arrangement.

Effect of *Sc*Zur Mutations on Target-Gene Expression. We then monitored the effect of mutations on the expression of three target genes of Zur. Transcripts from the *znuA* gene, encoding a component of zinc-uptake system, *rpmG2*, encoding a zinc-less paralog of ribosomal protein L33, and SCO7682, encoding coelibactin, were analyzed by S1 mapping. Fig. 3 shows representative results for three genes, indicated with average values obtained from three independent experiments. (The quantified data with SDs was presented in *SI Appendix*, Fig. S2.) The three genes were all derepressed in an *Δzur* mutant by 14-, 29-, and 33-fold, relative to the wild-type. Introduction of a wild-type *zur* gene to the *Δzur* mutant successfully repressed all gene expression. To our surprise, however, the effect of each mutation on repressing target genes was varied, depending on targets. The *znuA* gene expression was affected very sensitively by mutations, whereas *rpmG2* and SCO7682 were affected less sensitively. For example, 15 mutations affected *znuA* expression by more than twofold, whereas 8 or 9 mutations affected *rpmG2* or SCO7682 by more than twofold. In other words, transcription from the *znuA* gene responded more sensitively to changes in Zur than did the other two genes.

We categorized the mutations into three or four groups based on the extent of their effect. The critical residues that abolished Zur activity to derepress all three genes by more than 10-fold are Cys79 and Cys90, which constitute the C-site. Important residues that affected Zur activity in all three genes by more than twofold are Phe29, Arg77, His85, His87, Cys93, and Cys130. Cys133 mutation affected two genes. The rest (His36, Asp65, His84, His86, Glu98, and Glu105) affected only the *znuA* expression, implying that they serve a more subtle role in modulating Zur activity. Interestingly, the critical and important residues that affected all three genes constitute the M- or C-site, except Phe29 and Arg77, whereas the subtly modulating residues are at the D-site (His84, His86, Glu105), near the M-site (Glu98), or in the DB-domain (His36, Asp65). The effect of each residue on the function of Zur to enable sporulation and transcriptional regulation is summarized in *SI Appendix*, Table S2. The residues that affected all three genes also affected spore-formation.

Role of Each Metal-Binding Site. To delineate the role of each metal-binding site in forming an active Zur structure, we performed biochemical and spectroscopic analyses of wild-type and mutant Zur proteins. The C79S, C90S, and H84A mutants were examined as representatives of M-, C-, and D-site mutations, respectively. Gel permeation chromatography through a Superdex 75 column indicated that C90S variant does not form dimers, whereas others do (12) (*SI Appendix*, Fig. S3). Electrophoresis on SDS/PAGE also demonstrated that C90S variant does not form dimers (Fig. 4*A*). Circular dichroism spectroscopy revealed that

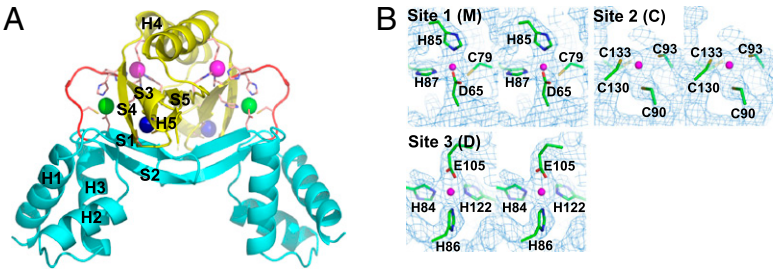

Fig. 1. Structure of *Sc*Zur. (*A*) Overall structure of *Sc*Zur determined at 2.4 Å resolution. The D- and DB-domains are colored by yellow and cyan, respectively. The hinge loop is in red. Zinc ions and metal-coordinating residues are represented by spheres and sticks, respectively. Pink, green, and blue spheres indicate zinc ions bound to the D-, M-, and C-sites, respectively. For clarity, secondary structure elements for one monomer are labeled. (*B*) Electron-density maps of three zinc-binding sites. Stereoview of the final $2F_o - F_c$ electron density maps contoured at 1σ, showing the M-, C-, and D-sites. Zn and Zn-coordinating residues are shown in spheres and sticks, respectively.

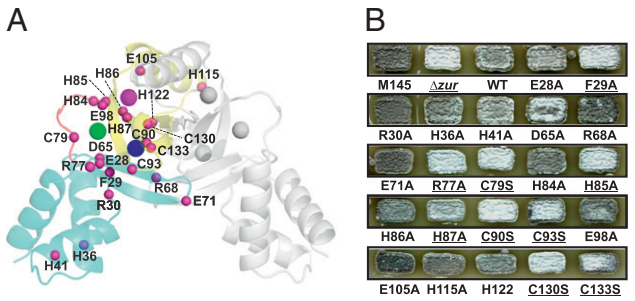

Fig. 2. Sporulation phenotype of various *zur* mutants. (*A*) The Cα atoms of 22 mutated residues are indicated as small spheres in 3D structure of *Sc*Zur drawn by transparent cartoon. Large spheres colored in pink, green, and blue represent zinc ions bound to the D-, M-, and C-sites, respectively. For clarity, one monomer is colored in white. The orientation is identical to Fig. 1*A*. (*B*) Activity of Zur variants to allow sporulation of *Δzur* mutant. About 1×10^5 spores of M145 (wild-type) and various Zur variant strains were streaked on SFM. Photos were taken at 7 d after inoculation. Mutants that do not restore sporulation remained white (underlined).

both the C79S and H84A mutants gave nearly identical spectra as the wild-type, whereas the C90S mutant gave a remarkably different spectrum (*SI Appendix*, Fig. S4). All these results indicate that the C90S mutation caused significant changes in secondary structure, consistent with the loss of dimerization. Therefore, zinc binding to the C-site serves a structural role. We then measured the metal content of various Zur preparations by inductively coupled plasma atomic emission spectroscopy (*SI Appendix*, Table S3). The average stoichiometry of zinc per monomeric Zur was 2.4 for the wild-type, 1.5 for H84A, 1.0 for C79S, 0.25 for C90S, and 1.2 for EDTA-treated apo-Zur. The observed amounts of zinc support the presence of more than two zinc-binding sites, structural importance of the C-site, and the more subtle role of the D-site compared with the M-site.

We then measured the ability of each Zur variant to bind different target promoter probes by EMSA. In addition to the three genes examined above, a probe for *rpmF2* that encodes a paralogue of ribosomal protein L32 was included in this assay. Plotting of the autoradiographic gel data (*SI Appendix*, Fig. S5) revealed characteristic binding curves (Fig. 4 *B–D*). The apparent binding affinity (K_D) of the wild-type, presented as the concentration of Zur at 50% up-shift of DNA probes, was stronger for *rpmG2* and SCO7682 (17.7 and 17.6 nM) than for *znuA* and *rpmF2* (74.9 and 68.3 nM) (Fig. 4*B* and *SI Appendix*, Fig. S5). The difference in DNA binding affinity parallels the differential sensitivity of gene expression to mutations in vivo (Fig. 3). The C79S mutation nearly abolished DNA binding to all promoters. On the other hand, the H84A mutation reduced DNA binding affinities of all promoters in the order of *rpmF2* (by 61-fold), SCO7682 (19-fold), *znuA* (11-fold), and *rpmG2* (7-fold). The sensitive promoter *rpmF2* was affected most, whereas the less sensitive promoter *rpmG2* was affected least. The results suggest that the H84A mutation can also affect the nearby M-site, but they clearly reveal the potential of modulating the D-site to achieve differential induction of target genes.

Differential Expression of Zur Target Genes on Zinc Depletion. We then explored whether each target gene responds to different concentrations of zinc. For this purpose, we treated cells with [N,N,N′,N′-Tetrakis-(2-pyridylmethyl) ethylenediamine] (TPEN), a potent zinc-chelator, at varying concentrations for 5 min, and analyzed transcripts by S1 mapping. The results in Fig. 5*A* demonstrate that *znuA* and *rpmF2* genes are induced at lower TPEN, reaching nearly full induction at 4 μM TPEN with about 93% of the maximal level at 50 μM treatment. In contrast, *rpmG2* and SCO7682 genes responded less sensitively to TPEN, with about 28% and 22% of full induction, respectively, at 4 μM TPEN. Even at 50 μM TPEN, 5-min incubation allowed only 65% and 48% of induction at 40 min, respectively. This differential zinc-dependent induction pattern echoes the differential sensitivity of promoters toward Zur mutations. We then examined the effect of TPEN on Zur-DNA binding in vitro. EMSA analysis revealed that Zur-DNA complexes on *znuA* and *rpmF2* promoters dissociated at lower TPEN (1.5–2 μM at 50% dissociation) than those on *rpmG2* and SCO7682 (5.6 μM TPEN) (Fig. 5 *B* and *C*). The EMSA results coincide with a differential gene-expression pattern in vivo, indicating that graded modulation of Zur activity by zinc lies behind differential expression of its targets.

Activation of Promoter-Binding Activities of Zur Occurs at Two Different Zinc Concentrations in Vitro. We then tried to estimate the zinc concentration ranges that Zur senses to regulate different genes. For this purpose, we determined the concentration of added zinc that conferred DNA-binding activity to apo-Zur that lacks regulatory metals because of EDTA treatment (*SI Appendix*, Table S3). DNA-binding curves were obtained for each promoter as a function of added $ZnSO_4$ in the presence of a metal buffer TPEN, as described by Outten and O'Halloran (4). Fig. 6 demonstrates clearly that binding to the two sets of promoters occurred at different zinc concentration ranges. Zur bound to the sensitive genes (*znuA*, *rpmF2*) at higher zinc (~3.8 μM at 50% binding) than to the others (at ~3.2 μM). In the presence of 5 μM TPEN, these values correspond to free-zinc concentrations of 7.8×10^{-16} M and 4.5×10^{-16} M, respectively, reflecting two different binding affinities to Zur (4) (www.stanford.edu/~cpatton/webmaxc/webmaxcS.htm). These values are comparable with the value (~0.2 fM) observed for *E. coli* Zur (4). However, it is evident in this study that ScZur responds to at least two different concentration ranges, albeit not drastically apart.

Discussion

Regulatory Role of M- and D-sites in Zur. Through mutation studies, we demonstrated that zinc binding to the C-site ensures dimeric structural integrity of Zur. This observation coincides with previous reports that zinc binding ensures dimeric structure for Fur from *E. coli* (25, 26) and that the Cys4-Zn site, which corresponds to the C-site, is critically required to maintain dimeric

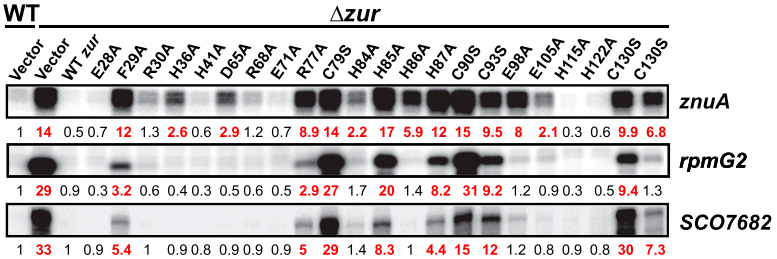

Fig. 3. Effect of various Zur mutations on the expression of three target genes in vivo. S1 mapping of *znuA, rpmG2* and SCO7682 transcripts. RNA samples for S1 mapping were prepared from the same strains used in Fig. 2. The amount of S1-protected band was presented relative to the level in wild-type (M145) cells containing parental vector (pSET162), as an average value from three independent experiments.

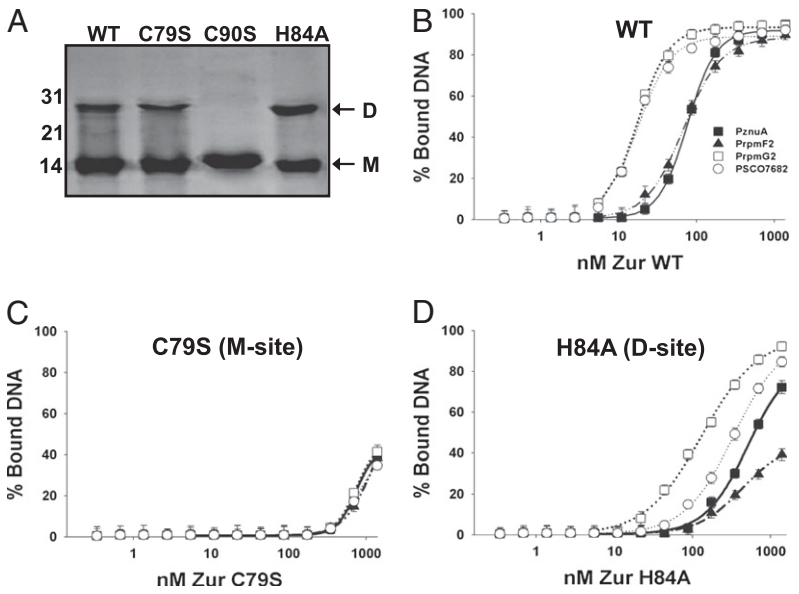

Fig. 4. Contribution of each metal-binding site on structural integrity and DNA-binding activity of *Sc*Zur. (*A*) Gel electrophoresis of purified Zur proteins. Wild-type and mutated Zur proteins (7 μg) were subjected to 13% SDS/PAGE. To visualize dimeric forms better, boiled samples in SDS-loading dye were mixed with nonboiled protein before loading. C79S, C90S, and H84A variants represent mutations in the M-, C-, and D-sites, respectively. (*B–D*) Zur-DNA binding was examined by EMSA for different Zur variants and promoters (*SI Appendix*, Fig. S5). Each labeled promoter probe of 100 bp (■ PznuA, ▲ PrpmF2, □ PrpmG2, and ○ PSCO7682) was incubated with increasing amounts of purified Zur of WT (*B*), C79S (*C*), and H84A (*D*) mutant form. A fraction of shifted (bound) DNA probes was plotted against Zur concentration, the plot was fit to a binding curve of Hill equation (connected lines).

structure of *Bs*PerR and Fur from *Helicobacter pylori* (*Hp*Fur) (27, 28). On the other hand, mutations at M- and D-sites did not affect dimerization as well as the characteristics of secondary structure. Therefore, it can be safely assumed that both M- and D-sites serve regulatory roles to modulate Zur activity. D-site occupation has been observed in *Pa*Fur (18) and *Vc*Fur (19). In these iron-responsive Fur proteins, the conserved C-terminal cysteines are lacking, and metals were found to occupy M- and D-sites. Because D-sites are occupied by zinc and M-sites can accommodate iron, the D-site in these proteins is regarded to serve a structural role. On the other hand, a recent report on the structure of active zinc-bound variant of *Hp*Fur, which contains C-terminal cysteines, revealed the occupation of the D-site in addition to M- and C-sites (29). In this structure, the D-site metallation has been proposed to be nonessential for DNA-binding, but to serve a secondary role to modulate binding affinity, consistent with what we discovered in the present study.

Although the domain structures of *Sc*Zur are virtually identical to those of *Mt*Zur, a remarkable difference exists between dimeric conformations of the two structures. *Sc*Zur assumes an arch-shaped DNA binding-competent closed conformation, whereas *Mt*Zur is reported to assume an inactive open conformation (20). In this context, the difference in metal content at the D-site between the two Zur proteins attracts our attention. According to the structural report of *Mt*Zur, a zinc ion at the D-site was refined with a low occupancy because of an initially high temperature factor (20). In contrast, the temperature factor and the occupancy of a zinc ion at the D-site in *Sc*Zur are comparable to those of coordinating residues, clearly indicating the presence of a zinc ion at the D-site. The fact that His84 in the hinge loop participates in metal coordination at the D-site (Fig. 1*A*) suggests that metal-binding to this site may affect the metal-induced swing motion of the DB-domain.

Based on our observations, we postulate a simplified model for modulating Zur activity through two regulatory zinc sites. Zinc binding to the M-site at the interdomain hinge loop activates Zur to bind its targets. Because the M-site has been revealed to accommodate various divalent cations, such as zinc, nickel, man-

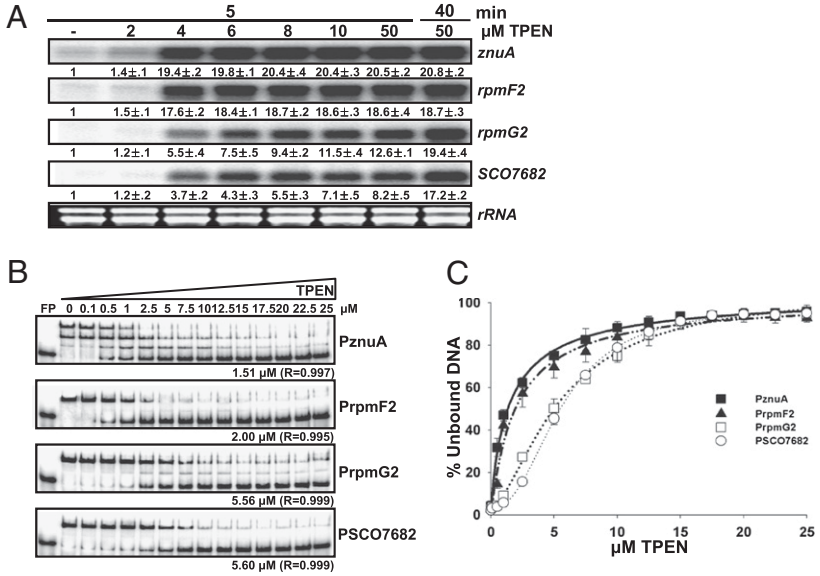

Fig. 5. Differential sensitivity of Zur target genes to zinc chelation in vivo and in vitro. (*A*) The wild-type cells grown in liquid YEME to early exponential phase were treated with various concentrations of TPEN from 2 to 50 μM (final) for 5 min, or for 40 min at 50 μM to allow full derepression. RNA samples were analyzed by S1 mapping. Average values from three independent experiments were indicated at the bottom of each lane, with the value of the nontreated sample set as 1.0. (*B* and *C*) Effect of TPEN on Zur-DNA binding in vitro. Each of four promoter DNA probes was incubated with WT-Zur (340 nM final) with increasing amounts of TPEN (0 to ~25 μM), and subjected to EMSA. Representative gel images with average K_D values (*B*) and binding curves (*C*) from three independent experiments are presented.

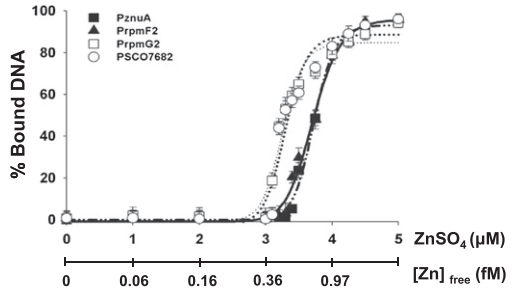

Fig. 6. Concentration ranges of zinc that activate Zur binding to different promoters. Each promoter DNA probe was incubated with EDTA-treated apo-Zur in the presence of varying amounts of $ZnSO_4$ (0–5 μM) and 5 μM TPEN in the binding buffer for 1 h. Following EMSA (*SI Appendix*, Fig. S6), the percent of bound DNA was plotted against added zinc, and the data were fit to the Hill equation. Average values with SDs were obtained from six independent experiments. The micromolar concentrations of $ZnSO_4$ at 50% binding were 3.83 ± 0.14 for *znuA*, 3.81 ± 0.16 for *rpmF2*, 3.25 ± 0.20 for *rpmG2*, and 3.26 ± 0.18 for SCO7682. The calculated concentration of free zinc was indicated in fentomolar on the parallel *x* axis.

ganese, and iron, in diverse active Fur family members (18, 19, 22, 23), it fits the previously proposed activation model (23). Without M-site occupation, Zur cannot bind and repress any of its target genes, causes disturbance in zinc homeostasis, and affects sporulation, most likely because of elevated synthesis of coelibactin (13). Nevertheless, it appears that M-site occupation may not be sufficient to guarantee binding to all target genes of Zur. The in vivo and in vitro observations that the D-site mutations affected target genes differently and that a higher amount of zinc was needed to allow Zur to bind to the more sensitive promoters (*znuA* and *rpmF2*) can be interpreted to imply that additional zinc binding to the D-site is needed to repress some targets, such as the sensitive group of genes. Therefore, in this model, the M- and D-sites can serve as an on-off switch and a tuner, respectively, for activity modulation. However, considering that Zur binds to its target sites with different affinity and that the presence of bound DNA can affect zinc-binding affinity of Zur, the more sensitive induction of a subset of genes upon smaller zinc depletion can be speculated to arise also from the weaker affinity of sensitive promoters to Zur. Even though the precise mechanism is currently beyond our understanding, the combined effect of two regulatory metal-binding sites and differential DNA-binding affinity of Zur seems to be behind the scenes. Even though we formulated the model based on negatively regulated target genes of Zur as a repressor, it can also be applied for positively regulated genes by Zur as an activator. No such gene has been reported yet in *S. coelicolor*, but we expect these genes exist, considering the example of positively regulated zinc-exporter gene by Zur in *Xanthomonas* (15).

Graded Expression of Metal-Sensitive Genes in Accordance with Metal Availability. The sensitive induction of a ZnuACB zinc transporter system and the ribosomal L32 paralog ahead of L33 paralog and coelibactin reflects the presence of a graded expression of metal-responsive genes in accordance with metal availability. The concentration range of free zinc, over which *Sc*Zur responds to modulate transcription of the four studied genes, spans from around 0.78 to 0.45 fM. Even though this is not a wide range, our finding clearly demonstrates that Zur differentially regulates its regulon members depending on the amount of available zinc. In *E. coli*, Zur responds to ∼0.2 fM of free zinc to regulate the zinc uptake gene (*znuC*), whereas ZntR responds to ∼1.2 fM zinc to regulate the zinc export gene (*zntA*) (4). This finding gives an idea about the range of free intracellular zinc over which *E. coli* responds to modulate its zinc-responsive factors. In *S. coelicolor*, no zinc export system has yet been reported, even though genome sequence predicts sequence homologs of ZntA, ZntR, and several P-type ATPases. Future studies on zinc-specific export systems and their regulators will provide complementing information on the range of zinc over which this organism responds to control transcription.

Behind the differential sensitivity of promoters to Zur activity modulation by zinc lie the differences in Zur-binding affinities of the two groups of promoters (Fig. 4*B*). We tried to find any characteristic sequence information in the promoter region, such as the number of and sequence similarity to consensus Zur-box (*SI Appendix*, Fig S7). No obvious sequence patterns correlated with binding affinities. Expression of different tiers of genes has been observed in a number of stress responses in response to the extent of stressors, such as heat and oxidants. However, in most cases the modulation is mediated by different sensor-regulators that detect different range or intensity of stimuli. For example, in *E. coli*, where heat-shock response is primarily mediated by a heat-shock σ factor RpoH (σ^{32}), heat at 42 °C increases the amount of RpoH to govern heat response, whereas extreme heat at around 50 °C requires an additional heat shock factor RpoE (σ^{24}) (30–32). In fission yeast *Schizosaccharomyces pombe*, responses to low and high levels of peroxide are modulated by Pap1 and Atf1, respectively (33). Differential activation of target genes by a single regulator (Zap1) in response to zinc deficiency has been reported in *Saccharomyces cerevisiae* (34), where the elucidation of an underlying mechanism is awaited. Activity modulation through two regulatory metal-binding sites in Zur extends the versatility of this regulator to allow graded expression of target genes in response to expanded concentration ranges of zinc. This mechanism will be beneficial for bacteria in all zinc-limiting environments, including those in animal hosts where zinc depletion is exploited as a defense mechanism against invading pathogens (35). There also remains a possibility that a similar principle abides in other metalloregulators, waiting to be examined.

Materials and Methods

Bacterial Strains and Culture Conditions. *S. coelicolor* strains M145 (wild-type), Δ*zur*, or Δ*zur* with chromosomally integrated *zur* gene (wild-type or site-specific mutant), were routinely grown in YEME liquid media with 10.3% sucrose (36). To cause zinc-depletion, various concentrations of TPEN were added at 2 to 50 μM (final) to exponentially growing cells in YEME for 5 or 40 min. For surface culture and to obtain spores, SFM media was used (36). For Δ*zur* mutants, which scarcely form spores, 30 SFM plates were grown to obtain about 5×10^8 spores, whereas only one SFM plate was sufficient to obtain 1×10^9 spores for wild-type strains. For PCR-targeted mutagenesis, *E. coli* BW25113 with pIJ790 plasmid were used as recommended (37). *E. coli* ET12567 with pUZ8002 plasmid were used for conjugal transfer (38).

Preparation of *Sc*Zur Proteins. Wild-type, C79S, C90S, and H84A mutant Zur proteins were purified from *E. coli* BL21 (DE3) cells containing pET3a-based recombinant plasmid, as previously described, with some modifications (12). EDTA was omitted in the buffer, except for preparing apo-Zur (*SI Appendix*). For gel electrophoresis to detect oligomerization status, samples of 7 μg each of purified Zur protein were used. Proteins boiled at 95 °C were mixed with the same amount of nonboiled proteins before 13% SDS/PAGE at 80 V (39).

Crystallization, Structure Determination, and Refinement. Crystals were obtained at 23 °C by the batch crystallization method with mother liquors of 15% PEG 3350 (wt/vol), 0.1 M magnesium formate, 0.1 M Bis-Tris (pH 6.5), and 0.8 mM CHAPSO. The crystals belonged to the space group *C*2 with cell parameters a = 103.6, b = 36.98, c = 71.65 Å, and β = 103.26°. For data collection, crystals were frozen at −170 °C after a brief immersion in a cryoprotectant solution containing 15% ethylene glycol in the same mother liquor. A 2.4 Å dataset (*SI Appendix*, Table S1) was collected at beamline 17A at Photon Factory. The model building was performed using COOT and refinement was done with a maximum-likelihood algorithm implemented in CNS (*SI Appendix*, Table S1). The structure was determined by molecular replacement using MolRep in the *CCP*4 program suite. Structures of DB- and D-domains in *Mt*Zur were separately used as search models. That is, two independent models were used to obtain phasing information. Several

rounds of refinement and remodeling produced a final model refined to R and R_{free} values to 21.4% and 24.9%, respectively.

Site-Specific Mutagenesis of *zur* and Introduction to Δ*zur* Cells. The template plasmid containing the entire coding region of *zur* was constructed in pGEM-Teasy vector (Promega), resulting in pSJ703. Site-specific mutagenesis was done with QuixChange mutagenesis kit (Stratagene). Twenty-two pairs of mutagenic primers were synthesized to change codons for cysteines to serines, and other amino acids to alanines. The mutated genes were verified by DNA sequencing, and recloned into pET3a (for pSJ704 series) and pSET162 (a derivative of pSET151, for pSJ705 series) plasmids for in vitro and in vivo studies, respectively. The final clones were confirmed again by DNA sequencing. The pSET162-based recombinant plasmids were introduced into Δ*zur* mutant of *S. coelicolor* by conjugal transfer, and the correct exconjugants were selected on antibiotics plates according to standard procedures (36). Each representative conjugant was isolated from a single colony, and confirmed by nucleotide sequencing of PCR products.

S1-Mapping Analysis. RNA samples were prepared from wild-type and Δ*zur* cells harboring chromosomally integrated copies of wild-type and mutated *zur* genes. Preparation of RNA, PCR amplification of gene-specific probes, radiolabeling of 5′ ends by ^{32}P, and S1-mapping analysis were done as described previously (12) and in the *SI Appendix*. Quantification of S1-protected bands was done through phosphor screen and image analyzer (FLA-2000; Fuji).

Zur-DNA Binding Analysis-EMSA. Each promoter DNA probe of ∼100 bp containing Zur binding sites was prepared by PCR, using primer pairs as detailed in *SI Appendix*, Fig. S7. Purified PCR products were labeled at 5′ ends with [γ-^{32}P] ATP using T4 polynucleotide kinase. The binding reaction was carried out by incubating ∼3.07 fmol of labeled DNA with varying amounts (6.8 fmol ∼27.84 pmol) of purified Zur proteins as isolated in 20 μL of binding reaction buffer [20 mM Tris-HCl (pH 7.8), 50 mM KCl, 1 mM DTT, 0.1 mg of BSA/mL, 5% glycerol, 0.1 μg of poly (dI-dC)] for 1 h at room temperature. For zinc-depletion experiments, further incubation with TPEN (up to 25 μM, 30 min) was carried out, followed by gel electrophoresis (12). For zinc-addition experiments, DNA probes were preincubated in binding reaction buffer with added $ZnSO_4$ (up to 5 μM) and 5 μM TPEN for 30 min before adding EDTA-treated apo-Zur (170 nM), followed by further incubation (1 h) and electrophoresis. The dried gels were exposed and quantified by a phosphorimage analyzer (BAS-2500; Fujifilm). We combined signals from all shifted bands for obtaining bound fraction, and the non-shifted band for nonbound fraction. Digitalized data were fit to binding curves through SigmaPlot 2001 program (SPSS Inc.). Apparent K_D values, corresponding to the concentration of variables (Zur, TPEN, or $ZnSO_4$) at half-maximal upshift of DNA probes, were determined from at least three independent sets of experiments.

ACKNOWLEDGMENTS. The authors thank Dr. Bairagi Mallick and Dr. Caryn Outten for circular dichroism spectroscopy and advice on free-zinc calculations, respectively. This work was supported by Grant NRF-2009-0079278 from the National Research Laboratory of Molecular Microbiology (to J.-H.R.); the Marine and Extreme Genome Research Center program, the Development of Biohydrogen Production Technology Using Hyperthermophilic Archaea program of the Ministry of Land, Transport, and Maritime Affairs, and the National Research Foundation of Korea Grant 2009-0084757 (to S.-S.C.); and a BK21 postdoctoral fellowship for Life Sciences at Seoul National University (to J.-H.S.).

1. Waldron KJ, Rutherford JC, Ford D, Robinson NJ (2009) Metalloproteins and metal sensing. *Nature* 460:823–830.
2. Andreini C, Bertini I, Cavallaro G, Holliday GL, Thornton JM (2008) Metal ions in biological catalysis: From enzyme databases to general principles. *J Biol Inorg Chem* 13:1205–1218.
3. Andreini C, Banci L, Bertini I, Rosato A (2006) Zinc through the three domains of life. *J Proteome Res* 5:3173–3178.
4. Outten CE, O'Halloran TV (2001) Femtomolar sensitivity of metalloregulatory proteins controlling zinc homeostasis. *Science* 292:2488–2492.
5. Giedroc DP, Arunkumar AI (2007) Metal sensor proteins: Nature's metalloregulated allosteric switches. *Dalton Trans* 29:3107–3120.
6. Hantke K (2005) Bacterial zinc uptake and regulators. *Curr Opin Microbiol* 8:196–202.
7. Akanuma G, Nanamiya H, Natori Y, Nomura N, Kawamura F (2006) Liberation of zinc-containing L31 (RpmE) from ribosomes by its paralogous gene product, YtiA, in *Bacillus subtilis*. *J Bacteriol* 188:2715–2720.
8. Maciag A, et al. (2007) Global analysis of the *Mycobacterium tuberculosis* Zur (FurB) regulon. *J Bacteriol* 189:730–740.
9. Nanamiya H, et al. (2004) Zinc is a key factor in controlling alternation of two types of L31 protein in the *Bacillus subtilis* ribosome. *Mol Microbiol* 52:273–283.
10. Owen GA, Pascoe B, Kallifidas D, Paget MS (2007) Zinc-responsive regulation of alternative ribosomal protein genes in *Streptomyces coelicolor* involves zur and sigmaR. *J Bacteriol* 189:4078–4086.
11. Panina EM, Mironov AA, Gelfand MS (2003) Comparative genomics of bacterial zinc regulons: Enhanced ion transport, pathogenesis, and rearrangement of ribosomal proteins. *Proc Natl Acad Sci USA* 100:9912–9917.
12. Shin JH, Oh SY, Kim SJ, Roe JH (2007) The zinc-responsive regulator Zur controls a zinc uptake system and some ribosomal proteins in *Streptomyces coelicolor A3(2)*. *J Bacteriol* 189:4070–4077.
13. Hesketh A, Kock H, Mootien S, Bibb M (2009) The role of *absC*, a novel regulatory gene for secondary metabolism, in zinc-dependent antibiotic production in *Streptomyces coelicolor A3(2)*. *Mol Microbiol* 74:1427–1444.
14. Kallifidas D, et al. (2010) The zinc-responsive regulator Zur controls expression of the coelibactin gene cluster in *Streptomyces coelicolor*. *J Bacteriol* 192:608–611.
15. Huang DL, et al. (2008) The Zur of *Xanthomonas campestris* functions as a repressor and an activator of putative zinc homeostasis genes via recognizing two distinct sequences within its target promoters. *Nucleic Acids Res* 36:4295–4309.
16. Lee JW, Helmann JD (2007) Functional specialization within the Fur family of metalloregulators. *Biometals* 20:485–499.
17. Cha SS, Shin JH, Roe JH (2010) *Sensing Metals: The Versatility of Fur in Bacterial Stress Responses* (ASM Press, Washington, D.C), 2nd Ed, pp 191–204.
18. Pohl E, et al. (2003) Architecture of a protein central to iron homeostasis: Crystal structure and spectroscopic analysis of the ferric uptake regulator. *Mol Microbiol* 47: 903–915.
19. Sheikh MA, Taylor GL (2009) Crystal structure of the *Vibrio cholerae* ferric uptake regulator (Fur) reveals insights into metal co-ordination. *Mol Microbiol* 72:1208–1220.
20. Lucarelli D, et al. (2007) Crystal structure and function of the zinc uptake regulator FurB from *Mycobacterium tuberculosis*. *J Biol Chem* 282:9914–9922.
21. An YJ, et al. (2009) Structural basis for the specialization of Nur, a nickel-specific Fur homolog, in metal sensing and DNA recognition. *Nucleic Acids Res* 37:3442–3451.
22. Jacquamet L, et al. (2009) Structural characterization of the active form of PerR: Insights into the metal-induced activation of PerR and Fur proteins for DNA binding. *Mol Microbiol* 73:20–31.
23. Giedroc DP (2009) Hydrogen peroxide sensing in *Bacillus subtilis*: It is all about the (metallo)regulator. *Mol Microbiol* 73:1–4.
24. Traoré DA, et al. (2006) Crystal structure of the apo-PerR-Zn protein from *Bacillus subtilis*. *Mol Microbiol* 61:1211–1219.
25. Pecqueur L, et al. (2006) Structural changes of *Escherichia coli* ferric uptake regulator during metal-dependent dimerization and activation explored by NMR and X-ray crystallography. *J Biol Chem* 281:21286–21295.
26. D'Autréaux B, et al. (2007) Reversible redox- and zinc-dependent dimerization of the *Escherichia coli* fur protein. *Biochemistry* 46:1329–1342.
27. Lee JW, Helmann JD (2006) Biochemical characterization of the structural Zn2+ site in the *Bacillus subtilis* peroxide sensor PerR. *J Biol Chem* 281:23567–23578.
28. Vitale S, et al. (2009) A ZnS(4) structural zinc site in the *Helicobacter pylori* ferric uptake regulator. *Biochemistry* 48:5582–5591.
29. Dian C, et al. (2011) The structure of the *Helicobacter pylori* ferric uptake regulator Fur reveals three functional metal binding sites. *Mol Microbiol*, 10.1111/j.1365-2958.2010.07517.x.
30. Raina S, Missiakas D, Georgopoulos C (1995) The *rpoE* gene encoding the sigma E (sigma 24) heat shock sigma factor of *Escherichia coli*. *EMBO J* 14:1043–1055.
31. Rouvière PE, et al. (1995) *rpoE*, the gene encoding the second heat-shock sigma factor, sigma E, in *Escherichia coli*. *EMBO J* 14:1032–1042.
32. Erickson JW, Gross CA (1989) Identification of the sigma E subunit of *Escherichia coli* RNA polymerase: a second alternate sigma factor involved in high-temperature gene expression. *Genes Dev* 3:1462–1471.
33. Quinn J, et al. (2002) Distinct regulatory proteins control the graded transcriptional response to increasing $H_{(2)}O_{(2)}$ levels in fission yeast *Schizosaccharomyces pombe*. *Mol Biol Cell* 13:805–816.
34. Wu CY, et al. (2008) Differential control of Zap1-regulated genes in response to zinc deficiency in *Saccharomyces cerevisiae*. *BMC Genomics* 9:370.
35. Kehl-Fie TE, Skaar EP (2010) Nutritional immunity beyond iron: A role for manganese and zinc. *Curr Opin Chem Biol* 14:218–224.
36. Kieser T, Bibb MJ, Buttner MJ, Chate KF, Hopwood DA (2000) *Practical Streptomyces Genetics*. (The John Innes Foundation, Norwich, United Kingdom).
37. Gust B, Challis GL, Fowler K, Kieser T, Chater KF (2003) PCR-targeted *Streptomyces* gene replacement identifies a protein domain needed for biosynthesis of the sesquiterpene soil odor geosmin. *Proc Natl Acad Sci USA* 100:1541–1546.
38. Mazodier P, Petter R, Thompson C (1989) Intergeneric conjugation between *Escherichia coli* and *Streptomyces species*. *J Bacteriol* 171:3583–3585.
39. Cortes DM, Perozo EP (1997) Structural dynamics of the *Streptomyces lividans* K^+ channel (SKC1): Oligomeric stoichiometry and stability. *Biochemistry* 36:10343–10352.